Dissolution Study of Lignin from Coconut Fiber as Lignocellulosic Biomass Using Eutectic Based Ionic Liquids

Ahmad Mudzakir*[1], Asep Bayu Dani Nandiyanto[1], Eddy Heraldy[2], Jon Efendi[3], Karina Mulya Rizky[1], Mia Widyaningsih[1] and Lewi Stefanus Anggiat[1]

[1] Universitas Pendidikan Indonesia, Bandung, Indonesia
[2] Universitas Sebelas Maret, Surakarta, Indonesia
[3] Universitas Negeri Padang, Padang, Indonesia
mudzakir.kimia@upi.edu

Abstract. Eutectic Based Ionic Liquids (EILs) are a new alternative to conventional ionic liquids which are considered cheaper, more environmentally friendly and biodegradable for use as a solvent in the chemical process of lignin. The aim of this research is to study the chemical process of lignin dissolution and delignification of biomass waste containing lignocellulose such as coconut fiber using cholinium chloride based EILs. The EILs were synthesized by a simple heating method using choline chloride with oxalic acid (CO) and ZnCl2 (CZ) . The synthesized EILs were then characterized using FTIR and NMR and their density was measured. The results show that the synthesized EILs have a density of 1.2864 g/cm3 and 1.7526 g/cm3 for CO and CZ EILs, respectively. FTIR and NMR studies on EILs confirmed that EILs were successfully synthesized. The solubility of synthesized EILs in lignin and cellulose was 42.03%; 5.44% and 32.51%; 7.73% for EILs CO and CZ respectively. The results of delignification of coconut fiber show that lignin from coconut fiber can be dissolved, indicated by changes in the color of EILs after delignification and separation. FTIR studies confirmed that the delignified lignin was shown to be at peak intensity in 1700-1400 cm-1 as the characteristic peak of lignin and NMR studies showed that there was a part of lignin that appeared in the NMR spectrum. The characteristics of coconut fiber after delignification show an increase in intensity for the functional groups present in cellulose, as shown by the FTIR results.

Keywords: Cholinium Chloride, Delignification, Eutectic Ionic Liquids, Lignin, Oxalic Acid, Zinc Chloride.

1 Introduction

Biolignocellulose is the most abundant source of renewable biomass in nature, but its commercial use value is much lower than expected even though biolignocellulose is a valuable chemical [1]. Bio lignocellulose can be used to produce fuel, chemicals and natural derivative materials that have added value. Bio lignocellulose is generally found in plant cell walls [2–5]. This characteristic is what makes researchers classify biomass

F. Khoerunnisa et al. (eds.), *Proceedings of the 9th Mathematics, Science, and Computer Science Education International Seminar (MSCEIS 2023)*, Advances in Social Science, Education and Humanities Research 860,
https://doi.org/10.2991/978-2-38476-283-5_33

as an alternative source of energy production that can meet global energy demand because biomass is a sustainable, renewable and environmentally friendly energy source such as sunlight, wind and water [6–9]. In this case, agricultural waste is a source of energy-producing biomass that is considered valuable [10, 11]. Biomass as an energy reserve for the environment takes up 12.83% of space and it is hoped that its use will continue for the next few decades [12].

Most biomass is produced from planting, harvesting, processing and consuming agricultural or agricultural products. The resulting residue is waste that has added value if it is processed properly and not just thrown away. Plant residues, which can be sourced from bananas, fruit peels, coconuts, rice husks, bagasse, corn cobs, and others, are materials that are suitable as sources for thermal and chemical processing [13–18]. The main components that form the cell walls of plants that produce lignocellulosic biomass are cellulose, hemicellulose and lignin [19].

Lignin is the second most abundant organic carbon after cellulose in the biosphere. Lignin has great potential as a substitute for natural oil-based materials and energy because of its chemical function. Apart from that, lignin also has the potential as an environmentally friendly raw material for adhesives, fertilizers, strengthening phases for polymer systems, substitutes for polymers from petroleum such as phenolic resins, adhesives and polyolefins, and others [20–26]. However, the complex structure of lignin makes its conversion and use as a good chemical a process that requires high costs and energy [27].

Over the past few years, ionic liquids have gained a lot of popularity and attention in this regard [28]; however, concerns regarding by-products resulting from pretreatment technologies, the high cost of ionic liquids and the unknown long-term toxicity of many of these solvents have been barriers to their scale-up and commercialization [29]. Therefore, eutectic ionic liquids (EILs) or also known as deep eutectic solvents (DES), as a new solvent that is environmentally friendly and inexpensive, has attracted much attention from researchers to overcome various problems with conventional ionic liquids (ILs). Similar to ILs, EILs have interesting properties including low volatility, non-flammability, high conductivity values, and many other unusual properties of these solvents [11].

EILs are a new generation of solvents designed to be environmentally friendly with lower costs and better environmental properties compared to conventional ionic liquids. Thanks to their excellent properties as solvents, they have been used for dissolution, pretreatment and chemical modification of lignocellulosic biomass [30–36]. The advantage of these EILs in lignocellulose compared to pretreatment with dilute acids is their ability to be used at high temperatures without requiring high pressure [37]. These EILs constitute a new group of solvents that can deconstruct biomass waste. On the other hand, these EILs/DES have also been successfully used in lignin solubilization in high yields using eutectic mixtures of cholinium chloride and hydrogen bond donors such as resorcinol and lactic acid. In treatment using EILs, a significant number of the main bonds in lignin can be broken down, resulting in a dissolved lignin fraction [13, 14, 38].

From previous research (Lian et al., 2015), DES type IV (hydrogen bond donor + metal halide) made from urea and zinc chloride can not only act as a solvent for lignin,

but also $ZnCl_2$ is integrated into the lignin. During the dissolution and subsequent precipitation of lignin, ZnO is formed in its polymer network, resulting in functionalizable products, however, the solubility of lignin in this particular DES is low due to the high viscosity of urea-zinc chloride DES at room temperature and its special solvation properties. In addition, the integration of Zn into lignin in the form of ZnO is limited to certain applications. To overcome these shortcomings, DES made from choline chloride and zinc chloride represent a better choice considering their lower viscosity and solvation properties (due to the presence of quaternary ammonium cations), which will allow for an increase in the amount of dissolved lignin without compromising the ability of DES to lignin functionalization (Abbott et al., 2005; Garcia et al., 2010), for example, utilizes Zn-based DES by fractionating/depolymerizing and oxidizing lignin in the presence of Lewis acidity provided by Zn (Abbott et al., 2001, 2002 ; Vigier et al., 2015) so that (i) Zn remains in the DES solvent after initial treatment (for example, DES can be regenerated) and (ii) the modified lignin can be easily recovered after the addition of antisolvent (for example, water).

In this research, two eutectic ionic liquids will be synthesized using ammonium cholinium chloride salt, with hydrogen bond donors and metal halides respectively, namely oxalic acid and $ZnCl_2$ with extraction capabilities for lignin. These two eutectic ionic liquids will be used as solvents for the delignification process of coconut fiber. The two synthesized eutectic ionic liquids were then characterized using ^{1}H NMR, ^{13}C NMR, FTIR, and their densities were measured. The synthesized ionic liquid was used further in the delignification process and studied in this research, and was further characterized using FTIR and NMR.

2 Method

The materials used in this research included choline chloride (Sigma Aldrich), zinc chloride (Sigma Aldrich), kraft alkaline lignin (Sigma Aldrich), PDB Broth [Potato Dextrose Broth] (HiMedia Laboratories), bacteriological agar no. 1 (Oxoid), anhydrous oxalic acid (Sigma Aldrich), local coconut fiber samples, distilled water, and technical grade methanol. All materials used are analytical grade and molecular biology grade unless stated.

2.1 Synthesis of Eutectic Ionic Liquids

Synthesis of eutectic ionic liquids is carried out using a simple heating method, namely each component of ammonium salt and hydrogen bond donor or metal halide is added to a Schlenk tube equipped with a magnetic stirrer and then heated on a hotplate with a sand bath at a temperature of 85-100 °C until a clear homogeneous liquid is formed. The synthesized EILs liquid was transferred to a vial, tightly closed and stored in a desiccator before and after being used for storage.

2.2 Density Measurement

The density of the synthesized EILs was determined using a pycnometer with a volume of 5 cm^3. The volume of the pycnometer was calibrated first using distilled water at 26 °C. The density of all EILs was measured by measuring the pycnometer in a water bath equipped with a thermometer. All EILs densities were measured at 26°C.

2.3 Measurement of Maximum Solubility of Kraft Lignin and Cellulose

Solubility determination was carried out for alkali kraft lignin and α-cellulose as a preliminary test to obtain information on the percent solubility of each constituent present in lignocellulose in all synthesized EILs. About 2–4% w/w of lignin and cellulose was added to 4 g of EILs. The percent solubility of lignin and cellulose is measured by weighing the dissolved mass of each constituent in a certain weight of the synthesized EILs using the equation 1.

$$\%\, Solubility = \frac{mass\ of\ dissolved\ constituents}{mass\ of\ EILs\ used} \times 100\% \quad (1)$$

2.4 Measurement of Maximum Solubility of Kraft Lignin and Cellulose

Coconut fiber samples were dried first for 1 hour using an oven at a temperature of 100 °C. The dried coconut fiber powder was ground using a blender, then the blended coconut fiber sample was further ground using a mortar and pestle. Samples of finely ground coconut powder were sieved using siever to a size of 140–200 mesh. The fine coconut fiber samples that had previously been sifted were then mixed with EILs (with a mass ratio of 1:20) in a Schlenk tube in a sand bath and heated at a temperature of 95–100°C for 24 hours. After the lignin extraction or delignification process is carried out for 24 hours, the solid residue and liquid fraction are separated using a centrifuge. Centrifugation was carried out at 3600 rpm for 20 minutes, the EILs fraction containing lignin was separated into closed vials referred to as LSKCO for the choline-oxalate (CO) EILs fraction containing lignin and LSKCZ for the choline-ZnCl2 (CZ) EILs fraction containing lignin. The solid residue was washed using methanol and then centrifuged again at 3600 rpm for 5 minutes several times until the solid residue washed with methanol was colorless. The solid residue that has been washed several times is dried in an evaporation cup and allowed to dry at room temperature for several hours and then heated for 1 hour in the oven. The dried solid residue is stored in a closed dry container and is referred to as SKCZ and SKCO for delignified solid residue using EILs CZ and CO, respectively.

2.5 Characterization

FTIR. Infrared spectra for all these samples were measured using an FTIR-8400S spectrometer (Shimadzu Europe). Infrared spectra were recorded over the range 4000 – 400 cm^{-1}.

NMR. NMR spectra were recorded using an Agilent 500 MHz spectrometer with a DD2 console system, operating at frequencies of 500 MHz for ^{1}H and 125 MHz for ^{13}C. Samples were measured using DMSO-d_6 solvent at sample amounts of 70-300 mg.

3 Results and Discussion

3.1 Synthesis of Eutectic Ionic Liquids

EILs consist of hydrogen bond acceptors and hydrogen bond donors. In this research, EILs were synthesized with ammonium salt cholinium chloride (ChCl) as a hydrogen bond acceptor (HBA) and ammonium salt. Choline chloride was chosen because of its good properties in interacting with lignin oligomers [11], while oxalic acid and zinc chloride ($ZnCl_2$) are used as hydrogen bond donors (HBD) and metal halides, respectively. The synthesis of EILs was carried out by heating the components for several hours at a temperature of 90°C accompanied by a stirring cycle of 500 rpm. The synthesis results show that EILs are in the form of a clear, thick, colorless homogeneous liquid with a characteristic odor. Fig. 1 shows the synthesis results of CO and CZ EILs.

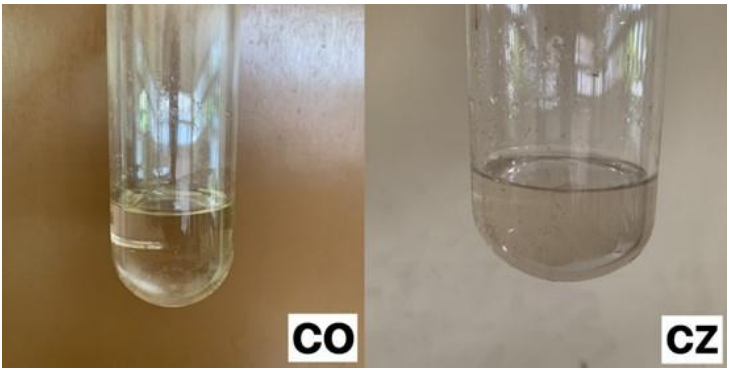

Fig. 1. Synthesis results of EILs CO (left) and CZ (right).

In this study, the molar ratios of the two EILs ChCl-oxalic acid (CO) and EILs ChCl-ZnCl2 (CZ) were 1:1 and 1:2, respectively. This selected molar ratio is the most commonly used ratio in many studies on EILs [39–41]. In CO EILs, a 1:1 ratio is used because oxalic acid is a dicarboxylic acid, which shows that for this system, eutectic occurs at 50% mole of the acid which can be achieved with a 1:1 ratio at which ratio the complex between the acid and the chloride ion occurs or can bridge acids between neighboring chloride ions [42]. Because the complex occurs in a 1:1 ratio, in this topic of delignification, a 1:1 ratio for EILs CO is a good ratio to be able to dissolve lignin in lignocellulosic materials. [11, 36]. In EILs CZ, a ratio of 2:1 is used because the mixture of cholinium chloride and zinc chloride has a eutectic composition at a molar ratio of 1:2, where at a mole fraction of 66-67%, both have a low freezing point compared to other ratios, so they are most suitable to be used in a 1:2 ratio [43].

Oxalic acid is used as a hydrogen bond donor because of its intermolecular forces which form a type of dipole-dipole attraction of hydrogen, especially hydrogen in the hydroxyl found in oxalic acid with the Cl- ion from choline chloride. Due to its acidic nature, strong hydrogen bonds will accept Cl- ions, so that when these strong hydrogen bonds are formed, the results will be effective in disrupting the intermolecular hydrogen bond network in the biomass and therefore can dissolve more lignocellulosic components [44, 45].

In the case of $ZnCl_2$, as a hydrogen bond acceptor, in EILs, intermolecular hydrogen bond interactions occur between Cl- ions as hydrogen bond acceptors and hydrogen from cholinium chloride as the donor. In addition, in previous research, $ZnCl_2$ and urea could not only dissolve lignin, but also $ZnCl_2$ was integrated into the lignin. Upon dissolution of lignin, ZnO is formed in the polymer network, producing a product that can be functionalized. Moreover, the mechanism of biomass delignification using DES is due to the ability of DES to selectively cut ether bonds between phenylpropane units in lignin without affecting the C-C bonds, while the use of $ZnCl_2$ as HBA in delignification only has a small effect on the substitution of aromatic rings in lignin, so it is good to use as a solvent in delignification [41, 46].

Density determination of both EILs was carried out to further characterize the synthesized EILs and confirm them by comparing the obtained density values with densities from the literature. From the results of density determination carried out using a distilled water calibrated pycnometer with a volume of 5 cm^3, the densities for EILs CO and EILs CZ are respectively 1.2864 g/cm^3 (26 °C) and 1.7526 g/cm^3 (26 °C). The density data for the CO EILs found are 1.282 g/cm^3 (25 °C) [47]. These differences cannot be compared directly because the two density values were measured at different temperatures. However, in general, the experimental density data carried out can confirm that EILs CO was successfully synthesized because the values only differ by around 0.004 g/cm^3. In addition, differences in these measurements can be caused by different instruments used to measure density. The density values from this experiment can confirm that CO EILs were successfully synthesized.

For CZ EILs, because the specific density data for EILs are very limited and varied, and data in the literature discussing the density of ChCl-$ZnCl_2$ EILs were not found, the density data from the above experiments cannot be compared. However, in general the density of EILs which have been reported to have a higher density than water is in the range of 1.0 to 1.6 g/cm^3, with EILs based on metal salts having density values in the range 1.3-1.6 g/cm^3 [48, 49]. From the high density for metal salts, this is expected given the high density of the experimental results (1.7526 g/cm^3 at 26 °C). The high density measured can probably be explained from the hole radius theory, when a density becomes high, the average hole radius decreases, thereby reducing the mass transport properties that can be carried out and ultimately increasing the viscosity. In research conducted by Abbott in 2004, the viscosity of EILs/DESs and ionic liquids was included in the hole theory model.

The void that results from a liquid when it melts has random sizes and its position is in constant motion. This theory states that an ion can only move in an ionic liquid if the ion is close to a hole of the same size or larger. Ionic liquids have high viscosity because the average size of an ion is 0.4 nm while the average hole radius is only about 0.2 nm.

Therefore, only a small fraction of the ions in an ionic liquid are moving at any one time due to the lack of holes of suitable size. From this theory, if we consider viscosity as a measure of the ease with which a species moves in a fluid, we would expect that fluids containing species of similar sizes, with similar densities, would have similar viscosities. Thus, the [Ch^+] cation present in the system is a cation with a smaller size than the cation found in the donor/ZnCl2 system in the literature (above it was mentioned that the density of EILs containing metal salts has a high value of 1.3-1.6 g/cm^3, where in this case it is urea/$ZnCl_2$ with the highest density of 1.6 g/cm^3 and urea is HBD, while $ZnCl_2$ is HBA), therefore, in this case where cholinium chloride is HBA, with the [Ch^+] cation having a larger size is small compared to urea, as a result it will have a higher viscosity, and because of the high viscosity, it would be expected that CZ EILs have a high density as well [50]. Table 1 summarizes well the synthesis and density determination results from these experiments.

Table 1. Synthesis Results and Density Determination

HBA/ Amonium Salts	HBD/Metal Halide	Molar Ratio	Physical Characteristics	ρa (g/cm3)
ChCl	Oxalic acid	1:1	Colorless homogeneous viscous liquid	1.2864
ChCl	ZnCl2	1:2	Colorless homogeneous viscous liquid	1.7526

[a]Experimental results measured at temperature 26 °C.

3.2 Measurement of Maximum Solubility of Kraft Alkali Lignin and Cellulose

The maximum amount of alkaline kraft lignin and cellulose for each synthesized EILs (CO & CZ) is shown in Table 2. The solubility of lignin in both EILs can be said to be quite good. Of the two synthesized EILs, EILs CO is better at dissolving lignin compared to EILs CZ as seen from the percent solubility, while the percent solubility of cellulose in both EILs can be said to be significantly low with a percent solubility below 10%. This shows that both EILs can be used as solvents that have great potential in dissolving lignin from lignocellulosic biomass.

Table 2. Maximum Solubility of Alkali Kraft Lignin and Cellulose in EILs

EILs	Alkali Kraft Lignin	Cellulose
CO (ChCl-Oxalic. Ac)	42.03%	5.44%
CZ (ChCl-ZnCl2)	32.51%	7.73%

Based on Table 2, CO EILs are almost 10% better at dissolving lignin. This can occur because the presence of hydrogen bonds in the eutectic solvent impacts the ether bonds in lignin, which reduces the energy required for their cleavage, and the lignin molecules will dissolve in the EILs [51]. The solubility of lignin in acidic EILs is higher than in basic EILs, because hydrogen bonds are stronger in acidic EILs. The hydrogen bond between the carboxylic acid and the chloride ion in EILs CO is a strong hydrogen

bond. However, it is interesting to note that on the contrary the solubility of cellulose is greater in CZ EILs than in CO EILs. In addition, this can occur because the carboxyl groups (-COOH) can easily react with the hydroxyl groups (-OH) on cellulose to form cross-linked monoesters or diesters. The diester formed can prevent cellulose from dissolving in acid hydrolysis and therefore increases the solubility of lignin [51]. The absence of a carboxyl group in $ZnCl_2$ to form a diester with cellulose is what causes the slightly higher solubility of cellulose in EILs CZ compared to EILs CO.

3.3 Delignification of Coconut Fiber

The result of delignification is in the form of two types of phases, namely the liquid phase and the solid phase. The liquid phase is EILs CO and CZ which contain the dissolved lignin fraction and are named respectively as LSKCO and LSKCZ, while the solid phase is the residual residue resulting from the separation of the dissolved lignin fraction in EILs (liquid phase) which is rich in cellulose (also known as cellulose rich residue). This solid residue is coconut fiber left over from delignification after drying. This solid residue is given the terms SKO and SKZ respectively for the remaining solid residue resulting from delignification by EILs CO and EILs CZ. Fig. 2 shows the physical form of the liquid phase and solid phase.

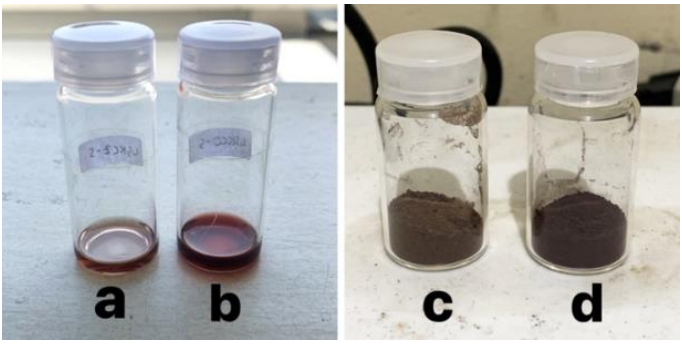

Fig. 2. Physical Forms of Liquid Phase (Left) and Solid Phase (Right) (a) LSKCZ, (b) LSKCO, (c) SKZ, and (d) SKO.

From the results of the synthesis and separation, the liquid phase containing lignin has a brownish color for LSKCZ and a dark red color for LSKCO. It should be noted that the two synthesized EILs are homogeneous colorless liquids, so this color change indicates that the EILs have successfully dissolved lignin. Lignin is a biomass that is rich in aromatic rings basically because it contains phenylpropane units. Lignin also contains functional groups that can absorb UV such as phenolics, ketones and other chromophores [52]. As we know, the part of the molecule that plays a role in the color of a compound is a chromophore, and this chromophore is a characteristic of the functional groups in lignin, including phenolics or ketones [53]. Chromophores in lignin generally include quinonoids, catechols, aromatic ketones, stilbenes, carbonyls conjugated with phenolics, and metal complexes [54].

In lignin, the contribution to color formation is mainly provided by the syringyl and guaiacyl units. Syringil absorption plays a role in forming a red-purple color at a wavelength of 270-273 nm, while the guaiacyl unit plays a role in forming a yellow-brown color because it can absorb UV light at a wavelength of 280-282 nm. The color of lignin depends on the color mixture of the chromophore groups that make it up [53]. Therefore, the occurrence of color changes in the liquid phase resulting from delignification after separation is initial evidence that lignin has been extracted and dissolved from coconut fiber.

3.4 FTIR Characterization

EILs CO. FTIR characterization was carried out to study and determine the changes that occur due to hydrogen bonds formed between choline chloride and hydrogen bond donors. Fig. 3 shows the FTIR spectra of the compounds choline chloride (ChCl), oxalic acid, and CO EILs.

In choline chloride, the broad peak in the region 3643–3255 cm^{-1} is a typical peak for the stretching hydroxyl (OH) group which is usually associated with the OH-Cl-group of choline chloride. The sharp peak at 1481 cm^{-1} is a typical peak for C-N bond stretching in choline chloride and is one of the characteristic features for identifying ChCl. Another sharp peak in choline chloride is the peak at 1085 cm^{-1} which indicates C-N vibrations. There is another typical peak that is correlated with choline chloride, namely a peak in the range 980-870 cm^{-1}, which appears right at the peak at 958 cm^{-1}, which is typical for quaternary ammonium, which is found in ChCl [55–57].

In oxalic acid, the characteristic peak is 3504-3420 cm^{-1} which indicates the stretching area of the OH group in oxalic acid, which is typical for carboxylic acids forming strong bonds in the dimer ring through intermolecular hydrogen bonds between C=O and the O-H group. The peaks 1617 cm^{-1} and 1255 cm^{-1} in oxalic acid were correlated with the stretching of C=O and C—O respectively which can be used to identify the presence of free oxalic acid in CO EILs. The next peak which is characteristic for oxalic acid is at 1438 cm^{-1} with this peak indicating the O—H bending group for carboxylic acid and the peak at 720 cm^{-1} is the peak for C=O stretching in oxalic acid [56, 58].

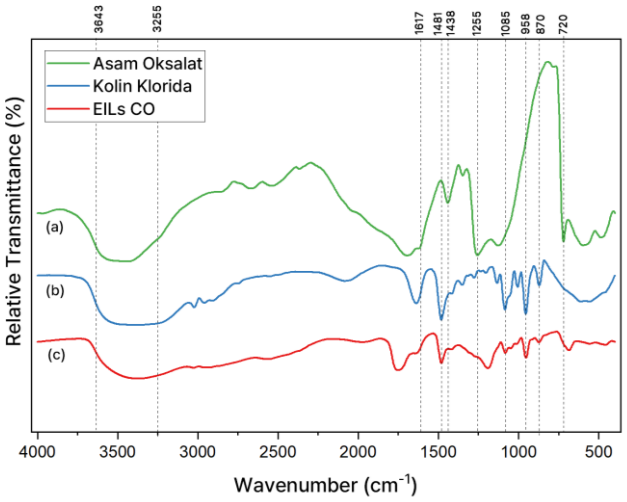

Fig. 3. FTIR spectra of (a) Oxalic Acid, (b) Choline Chloride, and (c) EILs CO.

The reappearance of these peaks as well as other peaks which may not have been mentioned but appear to have shifted, such as the peak at 685 cm^{-1} in EILs CO (Fig. 3), indicates a shift caused by the presence of hydrogen bonds formed between the constituents of EILs CO.

EILs CZ. Fig. 4 shows the FTIR spectra of $ZnCl_2$, choline chloride, and CZ EILs. As explained above, some of the peaks that have been described will be similar to the peaks in this spectrum. In the FTIR spectrum of choline chloride, the wide peak in the region 3643-3279 cm^{-1} indicates a stretching OH group, followed by a sharp peak at 1481 cm^{-1}. 1 is a typical peak for C-N bond stretching in choline chloride, another sharp peak in choline chloride is the peak at 1085 cm^{-1} which still indicates C-N vibrations. The peak at 958 cm^{-1} which is in the range 980-870 cm^{-1} remains characteristic of choline chloride, namely the peak for the presence of quaternary ammonium [55–57]. In the $ZnCl_2$ spectrum, the OH peak appears sharply at 3589 cm^{-1}, another characteristic appears at the peak at 1608 cm^{-1} which represents H-O-H bending which is the hydrate/hygroscopic nature of $ZnCl_2$. Metal halides show a peak at 750-100 cm^{-1}, in this spectrum the typical peak for metal halides is at 503 cm^{-1} which is correlated with Zn-Cl stretching [59].

The EILs CZ spectrum is a combination of both constituents. In EILs CZ, the OH group appears to appear in the form of a wide peak in the range of 3600-3200 cm^{-1}. The widening of this peak indicates that there are hydrogen bonds between donors and acceptors formed between ChCl and $ZnCl_2$. The peak at 1622 cm^{-1} is the peak for H—O—H bending which shifts from its constituents with peak sharpening, this phenomenon can be correlated with the formation of many strong O-H·O and O-H·Cl bonds in the CZ EILs. The peak for Zn-Cl experienced a shift in EILs CZ, which

appeared at the peak at 489 cm^{-1} [60]. This shift indicates the formation of hydrogen bonds between HBA and HBD [61].

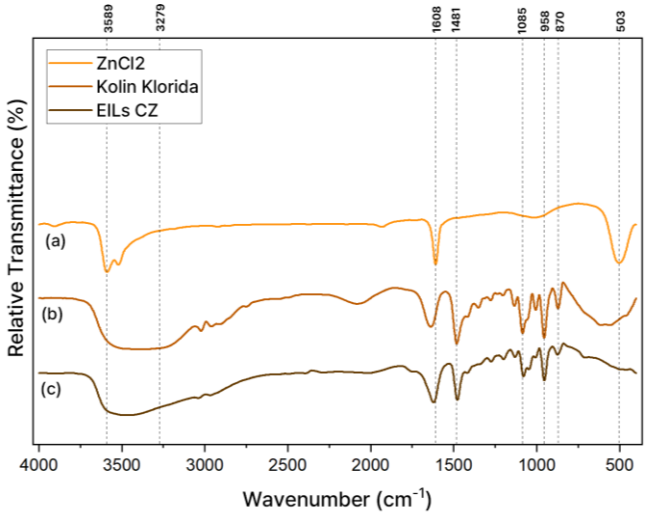

Fig. 4. FTIR spectra of (a) $ZnCl_2$, (b) Choline Chloride, and (c) EILs CZ.

LSKCO and LCO. FTIR spectra were taken on EILs containing the lignin fraction from delignification using EILs CO (LSKCO) to determine the presence of lignin from delignification in EILs CO, which was then compared with the FTIR spectra for EILs CO containing dissolved lignin (LCO). Fig. 5 shows the two spectra superimposed on each other with LSKCO given a black line and LCO as a comparison given a slightly transparent red line.

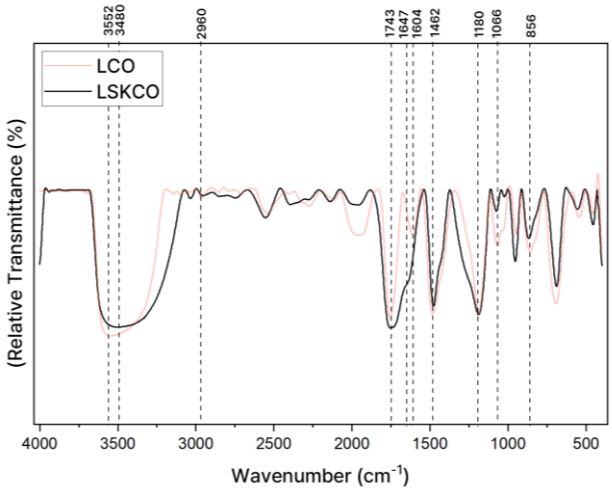

Fig. 5. LSKCO and LCO FTIR spectra.

From the spectra results, not much has changed in the peaks of the lignin structure, and almost all peaks appear in relatively the same area as EILs CO containing dissolved lignin (LCO), however in LSKCO it can be seen that several peaks have intensities that tend to be weaker . As shown in Fig. 5, the peak in the 3600-3300 cm^{-1} area is the peak for the hydroxyl group in both LCO and LSKCO. The peak for -CH stretching in both lignin in EILs is shown in the area (2960–2800 cm^{-1}) for stretching aliphatic chains and O-CH_3 groups, the characteristics of lignin are found in the benzene or aromatic ring framework of lignin which is depicted in the peaks in 1743, 1647, and 1462 cm^{-1}. The peak at 1463 cm^{-1} was correlated to C-H deformation combined with aromatic ring vibrations, indicating that the separated part was a lignin component. Therefore, the skeletal structure of the benzene ring is not destroyed and remains. The peaks at 1180 and 1066 are peaks that are respectively correlated with the guaiacyl ring because these peaks are peaks for C-O-C ether bonds and C-H bending vibrations in carbohydrates, which at the peaks are quite low, indicating the low content of carbohydrates and the purity of the extracted lignin is quite high. The next peak which is characteristic of lignin is at 856 cm^{-1} which is correlated with the vibration of C-H which is bound to the benzene ring [51, 62–64].

LSKCZ and LCZ. The FTIR spectra of EILs containing the lignin fraction resulting from delignification using EILs CZ (LSKCZ) were also compared with the FTIR spectra of lignin dissolved in EILs CZ (LCZ). Fig. 6 displays the FTIR spectra for LSKCZ and LCZ.

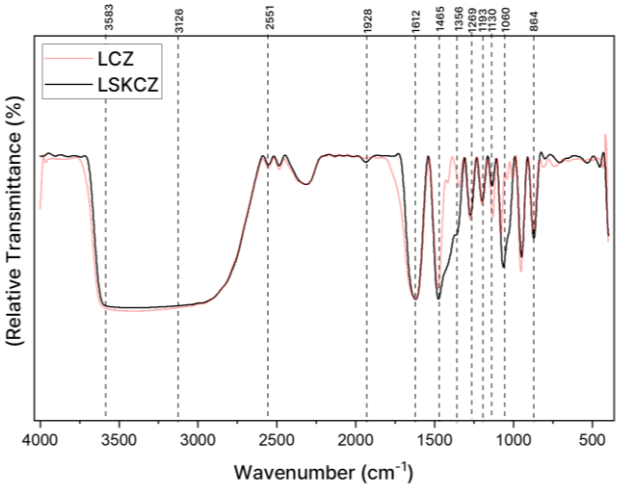

Fig. 6. FTIR spectra of LSKCZ and LCZ.

From the FTIR spectrum, similar to the previous one, there are not many peaks that change, in fact the peaks in LSKCZ tend to be almost entirely the same as the LCZ peaks, which is an initial indication that lignin is present in EILs CZ in the form of fractions as evidenced from this spectrum. The broad peak in the 3600-3100 cm^{-1} region

is completely correlated with the OH stretching group in both types of spectra which may result from some phenolics or aliphatics. The sharp peaks at 1612 cm^{-1}, 1465 cm^{-1} are characteristic of the characteristic framework for benzene or aromatic rings with their characteristic C=C vibrations. The peak at 2551 cm^{-1} is correlated to the alkane C-H stretching. The peak at 1356 cm^{-1} is weakly correlated to C-O stretching of the syringyl (S) region. Furthermore, the peak at 1269 cm^{-1} is the peak for the guaiacyl ring (G). The peak intensities at 1193 and 1130 cm^{-1} were attributed to the aromatic deformation of C-H in the S and G rings, and -O- in the ether, respectively. The region around 1193-820 cm^{-1} can indicate the presence of G, H, and S units. The weak peak at 1928 cm^{-1} can be correlated to unconjugated carbonyls indicating that to increase the phenolic hydroxyl content, the number of carbonyl groups from lignin is removed. during the delignification process using EILs CZ, and the peak at 864 cm^{-1} which is characteristic of the vibration of C-H bound to the benzene ring can be seen in both spectra [46, 51, 63, 64].

From the two FTIR spectra results in Fig. 5 and Fig. 6, it can be seen that the FTIR spectra for LSKCO and LSKCZ have peaks that tend to be similar to their respective counterparts, namely LCO and LCZ. The differences and shifts that occur can be correlated to the amount of lignin content which is different from its purity, different from the pure lignin content which has a better polymer or oligomer network without any bonds with lignocellulosic components such as in coconut fiber which is biomass.

SK, SKO, and SKZ. FTIR spectra were also taken in the residual solid phase resulting from delignification using EILs CO and CZ, which respectively are coconut fiber remaining from delignification and are named SKO and SKZ. Fig. 7 shows the FTIR spectra for coconut fibers that have not been delignified (SK), SKO, and SKZ.

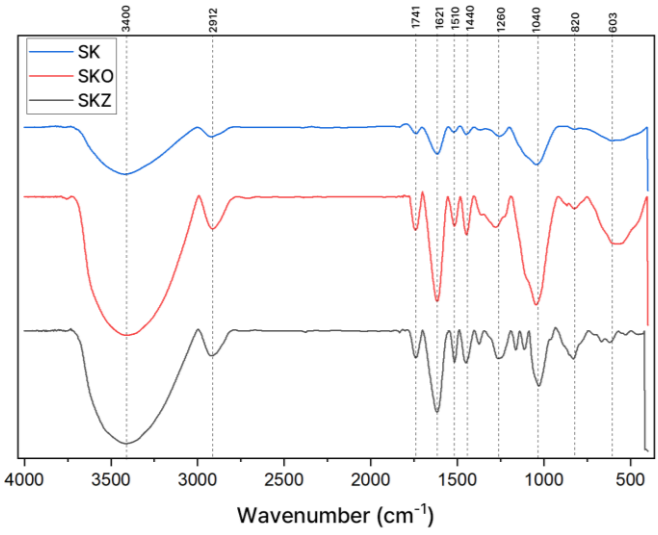

Fig. 7. FTIR spectra of SK, SKO, and SKZ.

From the spectra results above, the wide peak in the 3500-3300 cm^{-1} area, precisely at the 3400 cm^{-1} peak in the spectrum, describes the stretching vibrations of the hydroxyl groups in lignin or carbohydrates (cellulose or hemicellulose). The higher frequency of this area in SKO and SKZ compared to SK is a result of non-fiber material being removed and therefore more hydroxyl groups being produced. The peak at 2912 cm^{-1} is a peak that is correlated with C-H stretching and is very familiar to pyranoid rings in cellulose. The higher peaks in SKO and SKZ compared to raw SK indicate that EILs dissolve lignin well and not cellulose. The peak at 1741 cm^{-1} appears in the spectrum due to bending in water or it can also be correlated due to vibrations of the acetyl group on hemicellulose and the carboxyl group on lignin/hemiseulose. In general, the peak between 1650-1400 cm^{-1} is characteristic for the absorption of lignin. From the spectra it is known that in this area there are higher peaks for SKO and SKZ than for SK, this can occur due to the remaining solids/solid residues resulting from This delignification is also known as CRR or cellulose rich-residue which still allows residual lignin that cannot be extracted further, so it still appears as a peak. However, when compared with the lignin results in the previous section, it can be seen that this peak formed is not significant enough. The peak at 1260 is attributed to the C-O-C stretching of the glycosidic bonds of cellulose. The next peak is the high peak at 1040 cm^{-1}, this peak is correlated to the C-O-C vibration of the pyranose ring on cellulose or strong C-O-H stretching for cellulose. The last peak, namely the peak at 820 cm^{-1}, is the peak attributed to stretching vibrations for the beta 1,4-glycosidic bonds of hemicellulose. [45, 51, 65–70]. These spectra results show that the peaks that appear are mainly formed by cellulose or hemicellulose, which indicates that CO and CZ EILs can properly dissolve lignin from SK.

3.5 NMR Characterization

EILs CO. Fig. 8 shows the NMR spectra of the CO EILs. From the spectra it can be seen that the peaks of CH_2-N^+ in choline (b) and hydrogen -CH_3 in choline overlap, while the rest are separate and can be identified in the spectra of ^{1}H NMR (500 MHz, dmso) δ = 4.63 – 4.57 (d, *J*=4.9, 1H, H_d), 3.82 – 3.78 (s, 2H, H_h), 3.45 – 3.40 (t, *J*=5.1, 1H, H_c), 3.19 – 3.16 (s, 3H, H_b), 3.15 – 3.12 (s, 6H, H_g). In the spectrum of ^{13}C NMR (126 MHz, dmso) δ = 161.50 – 161.36 (C_f), 67.49 – 67.24 (t, *J*=2.8, C_b), 55.56 – 55.38 (C_c), 53.69 – 53.46 (t, *J*=3.8, C_a).

The occurrence of overlapping or slight displacement of the peak in ^{1}H NMR for EILs CO can occur due to dilution carried out using DMSO. However, from the spectra results it can be confirmed that EILs CO was successfully synthesized as indicated by the presence of all signals for each constituent that forms EILs CO.

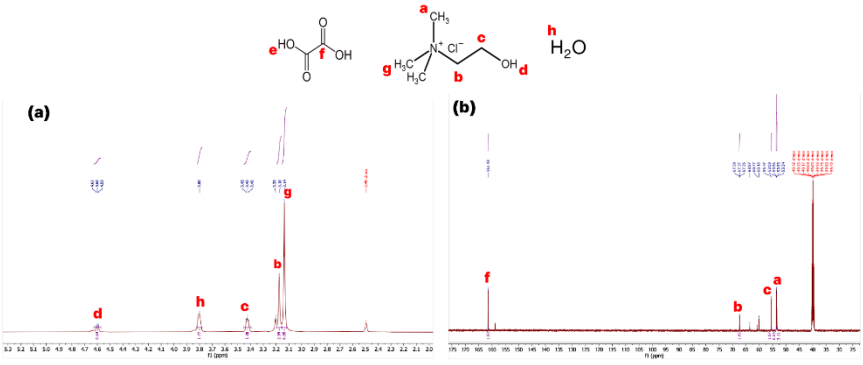

Fig. 8. Spectra of EILs CO ([Ch]Cl:OA): (a) ^{1}H NMR (b) ^{13}C NMR**.**

EILs CZ. Fig. 9 shows the expected NMR spectra of CZ EILs. All peaks are separate and identifiable for the spectrum of ^{1}H NMR (500 MHz, dmso) δ = 5.20 – 5.14 (t, *J*=4.9, 1H, H_d), 3.82 – 3.78 (s, 2H, H_c), 3.72 – 3.68 (s, 4H, H_f), 3.39 – 3.34 (t, *J*=5.1, 2H, H_b), 3.11 – 3.01 (s, 8H, H_e). The entire signal for ^{13}C NMR (126 MHz, dmso) also shows separate peaks, so it can be properly identified as follows δ = 67.56 – 67.35 (t, *J*=3.0, C_c), 55.74 – 55.59, C_b), 53.95 – 53.74 (t, *J*=3.8, C_a).

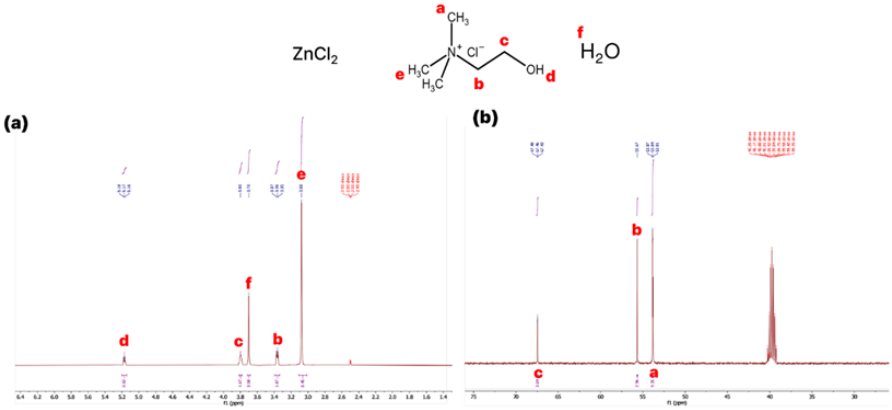

Fig. 9. Spectra of EILs CZ ([Ch]Cl:$ZnCl_2$): (a) ^{1}H NMR (b) ^{13}C NMR.

The occurrence of overlapping or slight displacement of the peak in ^{1}H NMR for EILs CO can occur due to dilution carried out using DMSO. However, from the spectra results it can be confirmed that EILs CO was successfully synthesized as indicated by the presence of all signals for each constituent that forms EILs CO.

This spectral peak was expected for the EILs CZ spectra because the peak signal for the $ZnCl_2$ constituent did not appear in the instrument used. From these results it can be confirmed that CZ EILs were successfully synthesized based on all signals that could be identified.

LSKCO. Fig. 10 shows the 1H NMR spectra for LSKCO. The peaks recorded for this spectrum are ^{1}H NMR (500 MHz, dmso) δ 6.73, 4.58, 3.80, 3.79, 3.44, 3.42, 3.42, 3.18. The peak with a shift of 6.73 ppm is correlated with aromatic H in the guaiacyl unit and aromatic H in the syringyl unit, 4.58 ppm for carbohydrates or H_{β} in β-O-4 structure, 3.80–3.42 ppm for H in the methoxyl present in the syringyl and guaiacyl units or methoxyl hydrogen in the aromatic part of the lignin substructure, and 3.18 is correlated to H_{β} in β-1 [71–73].

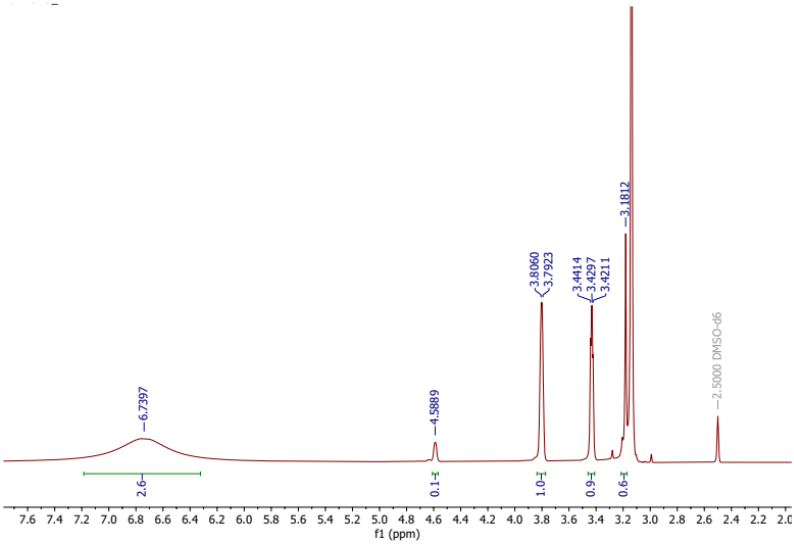

Fig. 10. Spectra of ^{1}H NMR LSKCO.

The ^{13}C NMR spectrum for LSKCO is shown in Fig. 11. The peaks recorded for this spectrum are ^{13}C NMR (126 MHz, dmso) δ 161.48, 159.01, 158.99, 67.38, 67.35, 67.33, 63.59, 60.00, 55.48, 53.61, 53.58, 53.55, 53.38, 40.28, 40.11, 40.03, 39.94, 39.87, 39.78, 39.70, 39.61, 39.44, 39.28. The peak with a shift of 161.48 ppm was correlated to the conjugated -COOH group of the unit in lignin or Benzoate C=O in *p*-OH-benzoate, a shift of 159.01–158.99 ppm was correlated to C_3, C_4 aromatic ether or hydroxyl or 4F in *p*-OH-benzoate. The shift at 67.38–63.59 ppm is correlated with aliphatic C_{α}-O or C-β, the β-1 structure of this shift can also be correlated with C-$_{\gamma}$ in the β-5 unit. The shift at 60.00–53.38 ppm is correlated with C methoxyl in the syringyl and guaiacyl units or C-β pinoresinol and phenylcoumaran, besides this shift can be correlated with C-$_{\gamma}$ in the β-O-4 unit and methoxyl in the syringyl and guaiacyl units [72, 74–76].

From the spectra results, some correlation for lignin appears in the peaks or signals, but further correlation is a limitation in these spectra because the spectra are produced from the lignin fraction and not lignin that has been further purified from the fraction. The few peaks that appear in these spectra indicate that good lignin dissolution occurs due to the strong hydrogen bonds between the solvent and most of the lignin [11].

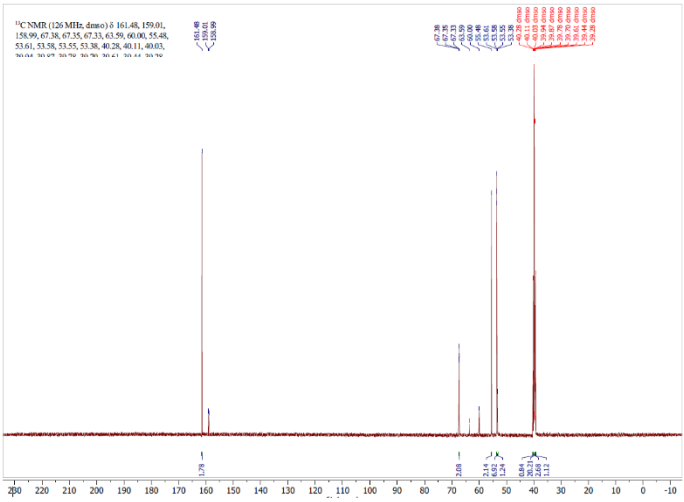

Fig. 11. Spectra of ^{13}C NMR LSKCO.

LSKCZ. Fig. 12 shows the ^{1}H NMR spectra for LSKCZ. The peaks recorded for this spectrum are ^{1}H NMR (500 MHz, dmso) δ 5.24, 5.23, 5.22, 3.83, 3.83, 3.82, 3.82, 3.81, 3.81, 3.80, 3.80, 3.79, 3.67, 3.39, 3.38, 3.38, 3.37, 3.37, 3.09, 2.50, 2.50, 2.50, 2.49, 2.49. The peak with a shift of 5.24 – 5.23 ppm is correlated with Benzylic OH in β-O-4 and β-1 or can also be correlated with H_α in the β-5 structure and noncyclic benzyl aryl ether, the shift at 3.83 – 3.37 ppm is correlated with H in the methoxyl present in the syringyl and guaiacil units or methoxyl hydrogens in the aromatic part of the lignin substructure, the peak in this shift can also be correlated with H-β on β-5 and H- ɣ on β-β, the shift at 3.23 – 3.09 ppm is correlated with Hβ hydrogen in the β-1 and β-β substructures, and the shift with a low peak at 2.50 – 2.49 ppm is correlated to the phenolic hydrogen OH or acetoxyl hydrogen in the aromatic part of the lignin substructure [71–73].

The ^{13}C NMR spectrum for LSKCZ is shown in Fig. 13. The peaks recorded for this spectrum are ^{13}C NMR (126 MHz, dmso) δ 67.28, 67.26, 67.24, 55.47, 53.61, 53.58, 53.55. The peak with a shift of 67.28 – 67.24 ppm is correlated with aliphatic Cα-O or C-β, the β-1 structure of this shift can also be correlated with C-ɣ in the β-5 unit. The shift at 55.47 – 53.55 ppm is correlated with C methoxyl in the syringyl and guaiacyl units or C-β pinoresinol and phenylcoumaran, besides this shift can be correlated with C-ɣ in the β-O-4 unit and methoxyl in the syringyl and guaiacyl units [72, 74–76].

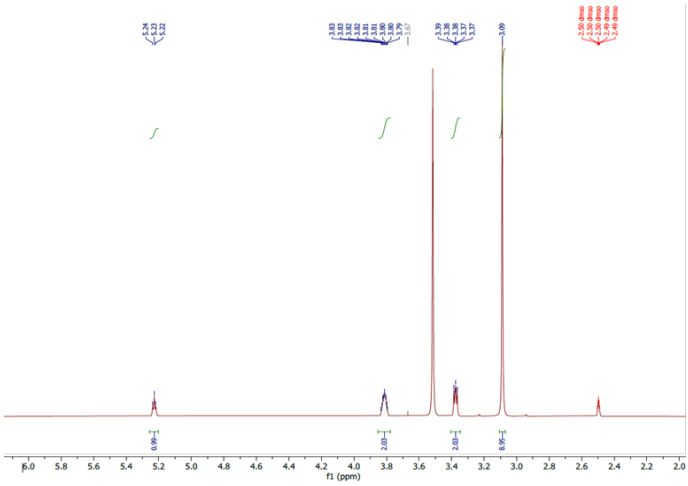

Fig. 12. Spectra of ^{1}H NMR LSKCZ.

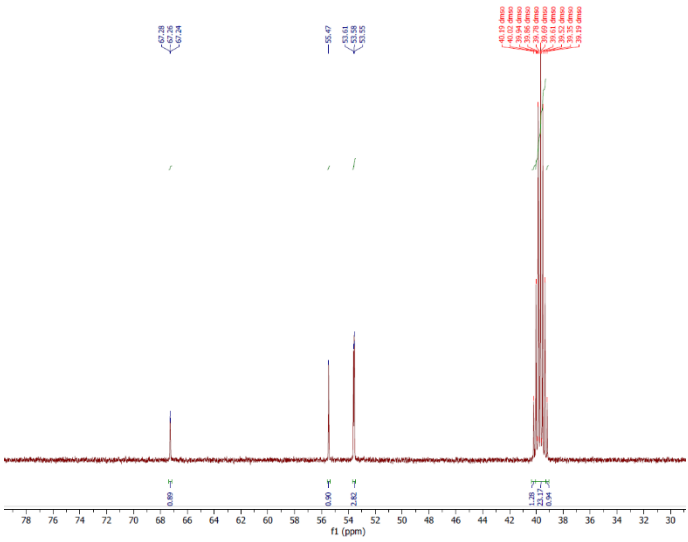

Fig 13. Spectra of ^{13}C NMR LSKCZ.

From the spectra results, some correlation for lignin appears in the peaks or signals, but further correlation is a limitation in these spectra because the spectra are produced from the lignin fraction and not lignin that has been further purified from the fraction. The few peaks that appear in these spectra indicate that good lignin dissolution occurs due to the strong hydrogen bonds between the solvent and most of the lignin [11].

4 Conclusion

Based on research that has been carried out, EILs cholinium chloride:oxalic acid (CO) [1:1] and cholinium chloride:$ZnCl_2$ (CZ) [1:2] have been successfully synthesized and have the form of a colorless, homogeneous viscous liquid. From the results of the FTIR study, the formation of hydrogen bonds and the combination of peaks of the constituent constituents were proven, and the NMR study also confirmed that both EILs were successfully synthesized. The respective densities for EILs CO and CZ are 1.2864 g/cm^3 and 1.7526 g/cm^3. The results of delignification of coconut fibers using EILs show that lignin has been successfully dissolved and extracted from coconut fibers, marked by a change in the color of the synthesized EILs to the color of EILs after delignification. EILs containing lignin from coconut fiber have similar characteristics in typical absorption peaks to EILs containing lignin alkaline kraft, with a higher lignin solubilizing ability for CO EILs. Lignin-containing EILs were also confirmed to contain various lignin components as indicated by NMR spectra. FTIR study of coconut fiber before and after delignification using EILs shows a higher intensity than before delignification, but this high result is dominated by functional groups from cellulose and not lignin.

References

1. Liu, W.-J., Jiang, H., Yu, H.-Q.: Thermochemical conversion of lignin to functional materials: a review and future directions. Green Chemistry **17**, 4888–4907 (2015).
2. Li, C., Zheng, M., Wang, A., Zhang, T.: One-pot catalytic hydrocracking of raw woody biomass into chemicals over supported carbide catalysts: simultaneous conversion of cellulose, hemicellulose, and lignin. Energy & Environmental Science **5**, 6383–6390 (2012).
3. Ragauskas, A.J., Williams, C.K., Davison, B.H., Britovsek, G., Cairney, J., Eckert, C.A., Frederick, W.J., Hallett, J.P., Leak, D.J., Liotta, C.L., Mielenz, J.R., Murphy, R., Templer, R., Tschaplinski, T.: The Path Forward for Biofuels and Biomaterials. Science **311**, 484–489 (2006).
4. Sanderson, K.: Lignocellulose: A chewy problem. Nature **474**, S12–S14 (2011).
5. Xia, Q., Chen, Z., Shao, Y., Gong, X., Wang, H., Liu, X., Parker, S.F., Han, X., Yang, S., Wang, Y.: Direct hydrodeoxygenation of raw woody biomass into liquid alkanes. Nature communications **7**, 11162 (2016).
6. Ayeni, A.O., Agboola, O., Daramola, M.O., Grabner, B., Oni, B.A., Babatunde, D.E., Evwodere, J.: Kinetic study of activation and deactivation of adsorbed cellulase during enzymatic conversion of alkaline peroxide oxidation-pretreated corn cob to sugar. Korean Journal of Chemical Engineering **38**, 81–89 (2021).
7. Ighalo, J.O., Adeniyi, A.G.: Factor effects and interactions in steam reforming of biomass bio-oil. Chemical Papers **74**, 1459–1470 (2020).
8. Rajendra, I.M., Winaya, I.N.S., Ghurri, A., Wirawan, I.K.G.: Pyrolysis study of coconut leaf's biomass using thermogravimetric analysis. IOP Conference Series: Materials Science and Engineering **539**, 012017 (2019).
9. Wang, Q., Sarkar, J.: Pyrolysis behaviors of waste coconut shell and husk biomasses. International Journal of Environmental Quality **3**, 34–43 (2018).

10. Adeniyi, A.G., Otoikhian, K.S., Ighalo, J.O., Mohammed, I.: Pyrolysis of different fruit peel waste via a thermodynamic model. ABUAD Journal of Engineering Research and Development **2**, 16–24 (2019).
11. Malaeke, H., Housaindokht, M.R., Monhemi, H., Izadyar, M.: Deep eutectic solvent as an efficient molecular liquid for lignin solubilization and wood delignification. Journal of Molecular Liquids **263**, 193–199 (2018).
12. Adewole, B.Z., Adeboye, B.S., Malomo, B.O., Obayopo, S.O., Mamuru, S.A., Asere, A.A.: CO-pyrolysis of bituminous coal and coconut shell blends via thermogravimetric analysis. Energy Sources, Part A: Recovery, Utilization, and Environmental Effects, 1–14 (2020).
13. Akond, A.U.R., Lynam, J.G.: Deep eutectic solvent extracted lignin from waste biomass: Effects as a plasticizer in cement paste. Case Studies in Construction Materials **13**, e00460 (2020).
14. Balasubramanian, S., Venkatachalam, P.: Valorization of rice husk agricultural waste through lignin extraction using acidic deep eutectic solvent. Biomass and Bioenergy **173**, 106776 (2023).
15. Li, X., Ning, C., Li, L., Liu, W., Ren, Q., Hou, Q.: Fabricating lignin-containing cellulose nanofibrils with unique properties from agricultural residues with assistance of deep eutectic solvents. Carbohydrate Polymers **274**, 118650 (2021).
16. Meraj, A., Singh, S.P., Jawaid, M., Nasef, M.M., Alomar, T.S., AlMasoud, N.: A Review on Eco-friendly Isolation of Lignin by Natural Deep Eutectic Solvents from Agricultural Wastes. Journal of Polymers and the Environment **31**, 3283–3316 (2023).
17. Panovic, I., Lancefield, C.S., Phillips, D., Gronnow, M.J., Westwood, N.J.: Selective Primary Alcohol Oxidation of Lignin Streams from Butanol-Pretreated Agricultural Waste Biomass. ChemSusChem **12**, 542–548 (2019).
18. Vargas Solis, D.C., Gorugantu, S.B., Carstensen, H.-H., Streitwieser, D.A., Van Geem, K., Marin, G.: Product distributions from fast pyrolysis of 10 Ecuadorian agricultural residual biomass samples. In: the 10th international conference on chemical kinetics (ICCK) (2017).
19. Osch, D.J.G.P. van, Kollau, L.J.B.M., Bruinhorst, A. van den, Asikainen, S., Rocha, M.A.A., Kroon, M.C.: Ionic liquids and deep eutectic solvents for lignocellulosic biomass fractionation. Physical Chemistry Chemical Physics **19**, 2636–2665 (2017).
20. Felby, C., Thygesen, L.G., Sanadi, A., Barsberg, S.: Native lignin for bonding of fiber boards—evaluation of bonding mechanisms in boards made from laccase-treated fibers of beech (Fagus sylvatica). Industrial Crops and Products **20**, 181–189 (2004).
21. Fischer, K., Schiene, R.: Nitrogenous Fertilizers from Lignins — A Review. In: Hu, T.Q. (ed.) Chemical Modification, Properties, and Usage of Lignin. pp. 167–198. Springer US, Boston, MA (2002).
22. Gosselink, R.J.A., Snijder, M.H.B., Kranenbarg, A., Keijsers, E.R.P., de Jong, E., Stigsson, L.L.: Characterisation and application of NovaFiber lignin. Industrial Crops and Products **20**, 191–203 (2004).
23. Ma, Y., Zhao, X., Chen, X., Wang, Z.: An approach to improve the application of acid-insoluble lignin from rice hull in phenol–formaldehyde resin. Colloids and Surfaces A: Physicochemical and Engineering Aspects **377**, 284–289 (2011).
24. Satheesh Kumar, M.N., Mohanty, A.K., Erickson, L., Misra, M.: Lignin and Its Applications with Polymers. Journal of Biobased Materials and Bioenergy **3**, 1–24 (2009).
25. Stewart, D.: Lignin as a base material for materials applications: Chemistry, application, and economics. Industrial Crops and Products **27**, 202–207 (2008).
26. Zhang, J., Chen, Y., Sewell, P., Brook, M.A.: Utilization of softwood lignin as both cross-linker and reinforcing agent in silicone elastomers. Green Chemistry **17**, 1811–1819 (2015).

27. Sun, N., Rodríguez, H., Rahman, M., Rogers, R.D.: Where are ionic liquid strategies most suited in the pursuit of chemicals and energy from lignocellulosic biomass? Chemical Communications **47**, 1405–1421 (2011).
28. Chatel, G., Rogers, R.D.: Review: Oxidation of Lignin Using Ionic Liquids—An Innovative Strategy to Produce Renewable Chemicals. ACS Sustainable Chemistry & Engineering **2**, 322–339 (2014).
29. Klein-Marcuschamer, D., Simmons, B.A., Blanch, H.W.: Techno-economic analysis of a lignocellulosic ethanol biorefinery with ionic liquid pre-treatment. Biofuels, Bioproducts and Biorefining **5**, 562–569 (2011).
30. Alvarez-Vasco, C., Ma, R., Quintero, M., Guo, M., Geleynse, S., Ramasamy, K.K., Wolcott, M., Zhang, X.: Unique low-molecular-weight lignin with high purity extracted from wood by deep eutectic solvents (DES): a source of lignin for valorization. Green Chemistry **18**, 5133–5141 (2016).
31. Cheng, F., Zhao, X., Hu, Y.: Lignocellulosic biomass delignification using aqueous alcohol solutions with the catalysis of acidic ionic liquids: A comparison study of solvents. Bioresource Technology **249**, 969–975 (2018).
32. Domínguez de María, P.: Recent trends in (ligno)cellulose dissolution using neoteric solvents: switchable, distillable, and bio-based ionic liquids. Journal of Chemical Technology & Biotechnology **89**, 11–18 (2014).
33. Francisco, M., van den Bruinhorst, A., Kroon, M.C.: Low-Transition-Temperature Mixtures (LTTMs): A New Generation of Designer Solvents. Angewandte Chemie International Edition **52**, 3074–3085 (2013).
34. Gunny, A.A.N., Arbain, D., Nashef, E.M., Jamal, P.: Applicability evaluation of Deep Eutectic Solvents–Cellulase system for lignocellulose hydrolysis. Bioresource Technology **181**, 297–302 (2015).
35. Smith, E.L., Abbott, A.P., Ryder, K.S.: Deep Eutectic Solvents (DESs) and Their Applications. Chemical Reviews **114**, 11060–11082 (2014).
36. Zhang, C.-W., Xia, S.-Q., Ma, P.-S.: Facile pretreatment of lignocellulosic biomass using deep eutectic solvents. Bioresource Technology **219**, 1–5 (2016).
37. Owhe, E.O., Kumar, N., Lynam, J.G.: Lignin extraction from waste biomass with deep eutectic solvents: Molecular weight and heating value. Biocatalysis and Agricultural Biotechnology **32**, 101949 (2021).
38. Muley, P.D., Mobley, J.K., Tong, X., Novak, B., Stevens, J., Moldovan, D., Shi, J., Boldor, D.: Rapid microwave-assisted biomass delignification and lignin depolymerization in deep eutectic solvents. Energy Conversion and Management **196**, 1080–1088 (2019).
39. Ijardar, S.P., Singh, V., Gardas, R.L.: Revisiting the Physicochemical Properties and Applications of Deep Eutectic Solvents. Molecules **27**, (2022).
40. Li, P., Zhang, Z., Zhang, X., Li, K., Jin, Y., Wu, W.: DES: their effect on lignin and recycling performance. RSC Advances **13**, 3241–3254 (2023).
41. Loow, Y.-L., New, E.K., Yang, G.H., Ang, L.Y., Foo, L.Y.W., Wu, T.Y.: Potential use of deep eutectic solvents to facilitate lignocellulosic biomass utilization and conversion. Cellulose **24**, 3591–3618 (2017).
42. Abbott, A.P., Boothby, D., Capper, G., Davies, D.L., Rasheed, R.K.: Deep Eutectic Solvents Formed between Choline Chloride and Carboxylic Acids: Versatile Alternatives to Ionic Liquids. Journal of the American Chemical Society **126**, 9142–9147 (2004).
43. Abbott, A.P., Capper, G., Davies, D.L., Rasheed, R.: Ionic Liquids Based upon Metal Halide/Substituted Quaternary Ammonium Salt Mixtures. Inorganic Chemistry **43**, 3447–3452 (2004).

44. Liu, Q., Zhao, X., Yu, D., Yu, H., Zhang, Y., Xue, Z., Mu, T.: Novel deep eutectic solvents with different functional groups towards highly efficient dissolution of lignin. Green Chemistry **21**, 5291–5297 (2019).
45. Ramesh, R., Nair, A., Jayavel, A., Sathiasivan, K., Rajesh, M., Ramaswamy, S., Tamilarasan, K.: Choline chloride-based deep eutectic solvents for efficient delignification of Bambusa bambos in bio-refinery applications. Chemical Papers **74**, 4533–4545 (2020).
46. Hong, S., Lian, H., Sun, X., Pan, D., Carranza, A., Pojman, J.A., Mota-Morales, J.D.: Zinc-based deep eutectic solvent-mediated hydroxylation and demethoxylation of lignin for the production of wood adhesive. RSC Advances **6**, 89599–89608 (2016).
47. Gontrani, L., Bonomo, M., Plechkova, N.V., Dini, D., Caminiti, R.: X-Ray structure and ionic conductivity studies of anhydrous and hydrated choline chloride and oxalic acid deep eutectic solvents. Physical Chemistry Chemical Physics **20**, 30120–30124 (2018).
48. Cui, Y., Li, C., Yin, J., Li, S., Jia, Y., Bao, M.: Design, synthesis and properties of acidic deep eutectic solvents based on choline chloride. Journal of Molecular Liquids **236**, 338–343 (2017).
49. El Achkar, T., Greige-Gerges, H., Fourmentin, S.: Basics and properties of deep eutectic solvents: a review. Environmental Chemistry Letters **19**, 3397–3408 (2021).
50. Abbott, A.P., Barron, J.C., Ryder, K.S., Wilson, D.: Eutectic-Based Ionic Liquids with Metal-Containing Anions and Cations. Chemistry – A European Journal **13**, 6495–6501 (2007).
51. Li, C., Huang, C., Zhao, Y., Zheng, C., Su, H., Zhang, L., Luo, W., Zhao, H., Wang, S., Huang, L.-J.: Effect of Choline-Based Deep Eutectic Solvent Pretreatment on the Structure of Cellulose and Lignin in Bagasse. Processes **9**, (2021).
52. Qian, Y., Qiu, X., Zhu, S.: Lignin: a nature-inspired sun blocker for broad-spectrum sunscreens. Green Chemistry **17**, 320–324 (2014).
53. Zhang, Y., Naebe, M.: Lignin: A Review on Structure, Properties, and Applications as a Light-Colored UV Absorber. ACS Sustainable Chemistry & Engineering **9**, 1427–1442 (2021).
54. Zhang, H., Fu, S., Chen, Y.: Basic understanding of the color distinction of lignin and the proper selection of lignin in color-dependent utilizations. International Journal of Biological Macromolecules **147**, 607–615 (2020).
55. Mulia, K., Krisanti, E., Terahadi, F., Putri, S.: Selected Natural Deep Eutectic Solvents for the Extraction of α-Mangostin from Mangosteen (Garcinia mangostana L.) Pericarp. International Journal of Technology **6**, 1211 (2015).
56. Saha, S.K., Dey, S., Chakraborty, R.: Effect of choline chloride-oxalic acid based deep eutectic solvent on the ultrasonic assisted extraction of polyphenols from Aegle marmelos. Journal of Molecular Liquids **287**, 110956 (2019).
57. Sivrikaya, S.: A novel vortex-assisted liquid phase microextraction method for parabens in cosmetic oil products using deep eutectic solvent. International Journal of Environmental Analytical Chemistry **99**, 1575–1585 (2019).
58. Muthuselvi, C., Arunkumar, A., Rajaperumal, G.: Growth and Characterization of Oxalic Acid Doped with Tryptophan Crystal for Antimicrobial Activity. Pelagia Research Library Der Chemica Sinica **7**, (2016).
59. Trivedi, M., Sethi, K., Panda, P., Jana, S.: A comprehensive physicochemical, thermal, and spectroscopic characterization of zinc (II) chloride using X-ray diffraction, particle size distribution, differential scanning calorimetry, thermogravimetric analysis/differential thermogravimetric analysis, ultraviolet-visible, and Fourier transform-infrared spectroscopy. International Journal of Pharmaceutical Investigation **7**, 33–40 (2017).

60. Deng, L., Jing, Y., Sun, J., Ma, J., Yue, D., Wang, H.: Preparation and properties of a moisture-stable ionic liquid ChCl–ZnCl2–MgCl2·2CH3COOCH2CH3·2H2O. Journal of Molecular Liquids **170**, 45–50 (2012).
61. Gautam, R., Kumar, N., Lynam, J.G.: Theoretical and experimental study of choline chloride-carboxylic acid deep eutectic solvents and their hydrogen bonds. Journal of Molecular Structure **1222**, 128849 (2020).
62. Li, P., Lu, Y., Li, X., Ren, J., Jiang, Z., Jiang, B., Wu, W.: Comparison of the Degradation Performance of Seven Different Choline Chloride-Based DES Systems on Alkaline Lignin. Polymers **14**, (2022).
63. Song, Y., Chandra, R.P., Zhang, X., Saddler, J.N.: Non-productive cellulase binding onto deep eutectic solvent (DES) extracted lignin from willow and corn stover with inhibitory effects on enzymatic hydrolysis of cellulose. Carbohydrate Polymers **250**, 116956 (2020).
64. Tian, D., Guo, Y., Hu, J., Yang, G., Zhang, J., Luo, L., Xiao, Y., Deng, S., Deng, O., Zhou, W., Shen, F.: Acidic deep eutectic solvents pretreatment for selective lignocellulosic biomass fractionation with enhanced cellulose reactivity. International Journal of Biological Macromolecules **142**, 288–297 (2020).
65. Abderrahim, B., Abderrahman, E., Aqil, M., Fatima Ezahra, T., Abdesselam, T., Krim, O.: Kinetic Thermal Degradation of Cellulose, Polybutylene Succinate and a Green Composite: Comparative Study. World Journal of Environmental Engineering **3**(4), 95-110 (2015).
66. Chen, W., He, H., Zhu, H., Cheng, M., Li, Y., Wang, S.: Thermo-Responsive Cellulose-Based Material with Switchable Wettability for Controllable Oil/Water Separation. Polymers **10**, 592 (2018).
67. Jia, N., Li, S.-M., Ma, M.-G., Zhu, J., Sun, R.-C.: Synthesis and characterization of cellulose-silica composite fiber in ethanol/water mixed solvents. Bioresources **6**(2), 1186-1195 (2011).
68. Kim, Y., Jeong, D., Park, K., Yu, J.-H., Jung, S.: Efficient Adsorption on Benzoyl and Stearoyl Cellulose to Remove Phenanthrene and Pyrene from Aqueous Solution. Polymers **10**, 1042 (2018).
69. Pokhrel, S., Shrestha, M., Slouf, M., Sirc, J., Adhikari, R.: Eco-Friendly Urea-Formaldehyde Composites Based on Corn Husk Cellulose Fiber. International Journal of Composite Materials **10**, 29–36 (2020).
70. Wulandari, W., Rochliadi, A., Arcana, I.M.: Nanocellulose prepared by acid hydrolysis of isolated cellulose from sugarcane bagasse. IOP Conference Series: Materials Science and Engineering **107**, 012045 (2016).
71. Chen, C.-L., Robert, D.: Characterization of lignin by 1H and 13C NMR spectroscopy. In: Methods in Enzymology, pp. 137–174. Academic Press (1988).
72. Lu, Y., Lu, Y.-C., Hu, H.-Q., Xie, F.-J., Wei, X.-Y., Fan, X.: Structural Characterization of Lignin and Its Degradation Products with Spectroscopic Methods. Journal of Spectroscopy **2017**, 8951658 (2017).
73. Lundquist, K.: Proton (1H) NMR Spectroscopy. In: Lin, S.Y. and Dence, C.W. (eds.) Methods in Lignin Chemistry, pp. 242–249. Springer Berlin Heidelberg, Berlin, Heidelberg (1992).
74. Mörck, R., Kringstad, K.P.: 13C-NMR Spectra of Kraft Lignins - II. Kraft Lignin Acetates **39**, 109–119 (1985).
75. Ralph, J., Landucci, L.L.: NMR of Lignins. In: Lignin and lignans: advances in chemistry, pp. 137–234. CRC Press (Taylor & Francis Group), Boca Raton, FL (2010).
76. Wang, K., Xu, F., Sun, R.: Molecular characteristics of Kraft-AQ pulping lignin fractionated by sequential organic solvent extraction. International Journal of Molecular Sciences **11**, 2988–3001 (2010).

.